

PACS numbers: 79.20.Ds; 42.55.Rz
DOI: 10.1070/QE2004v034n10ABEH002913

Effect of a target size on the recoil momentum upon laser irradiation of absorbing materials

A.N. Chumakov, A.M. Petrenko, N.A. Bosak

***Abstract*. The dependence of a recoil momentum on the radius of a target irradiated by a single-pulse Nd^{3+}:YAG laser ($\lambda = 1.064$ μm, $\tau = 20$ ns, $E \leqslant 300$ mJ) in the air is studied. The recoil momentum decreases three-fold with increasing the relative target radius from 0.3 to 5 and tends to saturation for $r > 3$. The calculation of the recoil momentum on the basis of the Euler and Navier – Stokes equations gave understated values for $r > 1$, which lowered to negative values. The reasons for the qualitative discrepancy between the experimental and calculated data is discussed.**

Keywords: *interaction of radiation with matter, laser-induced air breakdown, recoil momentum, ballistic pendulum.*

1. Introduction

A target irradiated by high-intensity laser radiation experiences a reactive recoil momentum arising from expanding vapour, which can be used to produce jet thrust [1]. The recoil momentum I is approximately proportional to the laser pulse energy E, making the specific recoil momentum I/E a convenient characteristic of laser radiation-to-mechanical energy conversion. The specific recoil momentum is maximal for some optimal value of the laser power density, which is about 0.5 GW cm^{-2} for metals irradiated in vacuum [2, 3]. For an evaporative thrust mechanism, the specific recoil momentum $I/E \approx 10$ dyn s J^{-1} and is primarily determined by the optical and thermodynamic properties of the target material [4 – 6].

With the discovery of a low-threshold optical near-target air breakdown by CO_2-laser radiation, a higher-efficiency explosion mechanism of pressure pulse transfer to the target was revealed [7 – 9]. In this case, the specific recoil momentum may five-fold exceed the specific evaporative momentum, ranging up to ~50 dyn s J^{-1}. This opens up the possibility of developing a laser-powered jet engine with air as the working medium [10 – 13]. Investigations revealed the dependence of recoil momentum on the shape and dimensions of the target [6, 9, 13 – 16]. The recoil momentum was shown to increase with target dimensions and then, on reaching its peak, to decrease slowly [13 – 16]. The momentum transfer from the near-surface plasma to the target is quite satisfactorily described by a spherical blast wave [17]. To analyse the resultant data, the target radius is conveniently expressed in relative units using its normalisation by the dynamic length $r_0 = (E/p_0)^{1/3}$, where p_0 is the normal atmospheric pressure. The previous experimental measurements of recoil momentum were performed for relative target radii $r \leqslant 1$, the greatest momentum being reached for $r \approx 0.3$ [16]. For these target radii, the results of measurements are in reasonable agreement with numerical simulations [18].

We have failed to find experimental data on the recoil momenta for targets with the radii $r > 1$. At the same time, numerical one-dimensional calculations [18, 19] were performed in a substantially broader range of target radii and testify to the change of sign of the recoil momentum with increasing radius above two dynamic units. Two-dimensional calculations of recoil momentum [20] carried out by the particle method in the case of a near-surface optical air breakdown have also led to negative values of recoil momentum with increasing the target radius. This is why of significant interest is the experimental determination of recoil momenta for large laser targets ($r > 2$) and their comparison with calculations.

2. Experimental

We used in our experiment a single-pulse 1.064-μm Nd:YAG laser emitting ~300-mJ, 20-ns pulses [21]. The laser radiation was focused onto the target with a spherical convex-plane lens with a focal length of ~60 mm to a spot 200 μm in diameter. The experiments were performed for an atmospheric air pressure. Brass foil disks were employed as the targets. Quantitative measurements were performed for a laser pulse energy of ~92 mJ. In this case, the laser energy density was ~300 J cm^{-2}. A near-surface air breakdown was initiated under these conditions, which was responsible for an almost complete absorption of laser radiation in the plasma produced.

The recoil momentum was measured by the pendulum technique. A brass target ~2 mm in diameter of mass ~40 mg was glued at the centre of a plastic disk attached to a free suspension with a length $l = 170$ mm which fulfilled the function of a pendulum. The plastic disks served as the receiving target area and were made of a thin and light yet rather rigid polymer film. The disk radius ranged from 0.2 to

A.N. Chumakov, A.M. Petrenko, N.A. Bosak Institute of Molecular and Atomic Physics, National Academy of Sciences of Belarus, prosp. F. Skoriny 70, 220072 Minsk, Belarus; Fax: 284 00 30; web-site: http://imaph.bas-net.by

Received 19 December 2003; revision received 6 August 2004
Kvantovaya Elektronika **34** (10) 948 – 950 (2004)
Translated by E.N. Ragozin

5 cm. Their masses m were measured with an ADV-200-M analytical balance with an uncertainty of 0.1 mg and were found to range between 40.7 and 536.0 mg, respectively. The horizontal pendulum deviation x from the equilibrium position was visually determined with the aid of a measuring microscope. The recoil momentum I was determined from the horizontal pendulum deviation using the relation

$$I = mx\left(\frac{g}{l}\right)^{1/2}, \tag{1}$$

where g is the acceleration of gravity. For every selected target radius, we performed a series of measurements to determine the average value of I. Relation (1) neglects the target deceleration in the air. However, it provided sufficiently accurate values of I, because the velocities of target motion were low under our experimental conditions.

The gas dynamic processes in the optical breakdown were numerically simulated by solving the problems on the decay of a spherical discontinuity for the gas dynamic Euler equations and the Navier–Stokes equations for a compressible gas whose viscosity was assumed to be equal to the viscosity of air. Both problems (for the ideal and viscous gases) were assumed to be spherically symmetric and were treated in the Lagrangian physical coordinates. Our technique is distinguished for the use of fully conservative difference schemes as the heart of the computational algorithm. The calculations were performed with the aid of the code package of Ref. [22]. In our formulation of the problem, the target was assumed to reside in the plane of symmetry. The recoil momentum was determined from the relation [23]

$$I(r) = 2\pi \int_0^r \int_0^\infty (p - p_0)\mathrm{d}t r\mathrm{d}r. \tag{2}$$

In the comparison with experiment, account should be taken of the fact that relation (2) neglects the flow that reaches the rear side of the target when the compression wave reaches its edge.

3. Results and discussion

The experimental values of recoil momentum are given in Fig. 1. They were measured for target radii in the range between 0.2 and 5 dynamic units. Also given here are the experimental data of Ref. [16] obtained earlier for target radii $r < 0.6$. Dependence (*3*) was derived in the solution of the Euler equations and dependence (*4*) in the solution of the Navier–Stokes equations. In the construction of these dependences we included the correction for the flow-bending effect. It was determined from the following considerations. The flow bending round the target is responsible for a pressure rise at its rear side and thereby retards its motion and decreases the experimental recoil momentum. That is why one-dimensional calculations, which do not take into account this flow bending, yield values of recoil momentum overestimated in comparison with the experimental ones, as indicated in Ref. [16]. An analysis of the calculated and experimental data for small target radii suggests that the contribution to the recoil momentum made by the explosion flow that reaches the rear side of the target is similar to the contribution of the flow at its facial side, with a similarity coefficient smaller than unity, but is opposite to it in sign. In our case, the greatest calculated recoil momentum was almost two times greater than the measured one, and therefore the similarity coefficient was taken to be equal to 0.5. The bent-flow contribution estimated in this way was subtracted from the calculated values of recoil momentum.

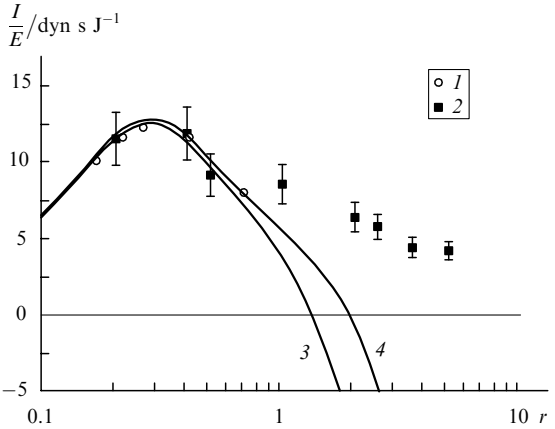

Figure 1. Specific recoil momentum I/E as a function of the target radius r normalised to the dynamic length: (*1*) experimental data of Ref. [16]; (*2*) data of the present work; (*3*) calculations by the Euler equations; (*4*) calculations by the Navier–Stokes equations.

The calculated dependences thus constructed agree nicely with the experimental ones throughout the $r < 0.6$ range. All the dependences have maxima at $r \approx 0.3$. The maximum measured values is $I/E \simeq 12.7$ dyn s J^{-1}. The sharp decrease of the experimental dependence for $0.3 < r < 0.6$ gives place to its slow decrease, which is concluded with a positive plateau with $I/E \approx 4.2$ dyn s J^{-1} for $r > 3$. By contrast, the calculated dependences drop to negative values for $r > 1$, despite the neglect of decelerating action of the flow which bends into the domain behind the target. The inclusion of viscous dissipation in the air brings the calculated dependence of the recoil momentum on r [curve (*4*)] somewhat closer to the experimental one but does not eliminate the qualitative difference between them.

This discrepancy between the experimental and calculated recoil momenta for large target dimensions should stem from the difference between the corresponding pressure pulses. Our experiments did reveal slowly decaying quasi-periodic oscillations of the pressure pulse, which were absent in the calculations [24]. At the same time, the pressure amplitudes and the arrival times of the real and calculated shock waves are in reasonable good agreement [25].

In our view, the uncovered pressure pulsation arises from the transformation of shock-wave perturbation to the acoustic radiation, which is disregarded in the gas-dynamic description of the explosion. This transformation is due to the acoustic dispersion and possesses a threshold. Most likely it sets in together with the formation of the region of reverse flow, when the distance of the shock front to the centre is $r > 0.6$. The transformation is accompanied with the energy transfer from the shock-wave perturbation to the acoustic radiation and is responsible for the moderation of the decrease of the experimental dependence of the recoil momentum on r compared to the calculated one. The acoustic radiation does not lead to mass transfer and cannot exert effect on the magnitude of recoil momentum, and

therefore the recoil momentum achieves a plateau on completion of such transformation.

4. Conclusions

The results obtained in our work allow the following conclusions:

(1) The experimental recoil momentum is positive for targets of arbitrary size and exhibits a slight dependence on their radius, which is of significance for the development of laser-powered jet engines.

(2) The qualitative difference between the experimental and calculated recoil momenta for large target dimensions can be attributed to the transformation of the shock-wave perturbation to the sound pulse at the late stage of the breakdown, which the calculations do no take into account.

Acknowledgements. This work was supported by the Belorussian Foundation for Basic Research (Contract No. F03-251).

References

1. Askar'yan G.A., Moroz E.M. *Zh. Eksp. Teor. Fiz.*, **43** (6), 2319 (1962).
2. Gregg D.W., Thomas S.J. *J. Appl. Phys.*, **37**, 2787 (1966).
3. Bonch-Bruevich A.M., Imas Ya.A. *Zh. Tekh. Fiz.*, **37**, 1917 (1967).
4. Kantrowitz A.R. *Astronautics and Aeronautics*, **9** (3), 34 (1971).
5. Kantrowitz A.R. *Astronautics and Aeronautics*, **10** (5), 74 (1972).
6. Pirri A.N., Monsler M.J., Nebolsine P.E. *AIAA J.*, **12** (9), 1254 (1974).
7. Pirri A.N., Schlier R., Northam D. *Appl. Phys. Lett.*, **21** (3), 79 (1972).
8. Pirri A.N. *The Physics of Fluids*, **16** (9), 1435 (1973).
9. Barchukov A.I., Bunkin F.V., Konov V.I., Prokhorov A.M. *Pis'ma Zh. Eksp. Teor. Fiz.*, **17** (8), 413 (1973).
10. Pirri A.N., Weiss R.F. *AIAA Paper*, (72), 719 (1972).
11. Barchukov A.I., Bunkin F.V., Konov V.I., Prokhorov A.M. *Pis'ma Zh. Eksp. Teor. Fiz.*, **23** (5), 273 (1976).
12. Korobeinikov V.P. *Inzh.-Fiz. Zh.*, **25**, 1121 (1973).
13. Bunkin F.V., Prokhorov A.M. *Usp. Fiz. Nauk*, **119** (3), 425 (1976).
14. Ageev V.P., Barchukov A.I., Bunkin F.V., Konov V.I., Silenok A.S., Chapliev N.I. *Kvantovaya Elektron.*, **4** (2), 310 (1977) [*Sov. J. Quantum Electron.*, **7** (2), 171 (1977)].
15. Ageev V.P., Burdin S.G., Goncharov I.N., Konov V.I., Minaev I.N., Chapliev N.I. *Vzaimodeistvie moshchnogo lazernogo izlucheniya s tverdymi telami v gazakh* (Interaction of High-Power Laser Radiation with Solids in Gases) (Itogi Nauki i Tekhniki. Ser. Radiotekhnika. Moscow: VINITI, 1983) Vol. 31.
16. Kozlova N.N., Petrukhin A.I., Pleshanov Yu.E., Rybakov V.A., Sulyaev V.A. *Fizika Goreniya i Vzryva*, **11** (4), 650 (1975).
17. Kuriki K.. Kitora Y. *Appl. Phys. Lett.*, **30** (9), 443 (1977).
18. Okhotsimskii D.E., Kondrasheva I.L., Vlasova Z.P., Kazakova R.K. *Trudy Matemat. Inst. AN SSSR*, **50**, 3 (1957).
19. Broud G. *Computer Simulations of Explosions. Mechanics Ser. News of Foreign Science* (Moscow: Mir, 1976).
20. Stankevich Yu.A. *Abstract of Thesis for Candidate's Degree* (Minsk: Institute of Physics, Belorussian Academy of Sciences, 1982).
21. Efremov V.V., Tylets N.A. Chumakov A.N., Shienok Yu.F. *Prib. Tekh. Eksp.*, (4), 179 (1992).
22. Petrenko A.M. *Algoritm. Program. Inf. Byul.*, (11), 4 (1988).
23. Kovaleva I.N., Nemchinov I.V. *Fiz. Goren. Vzryv.*, **12** (1), 113 (1976).
24. Chumakov A.N., Petrenko A.M., Bosak A.N. *Inzh.-Fiz. Zh.*, **76** (4), 89 (2003).
25. Chumakov A.N., Petrenko A.M., Bosak A.N. *Inzh.-Fiz. Zh.*, **75** (3), 89 (2002).